

Pros and Cons of Rotating Ground Motion Records to Fault-Normal/Parallel Directions for Response History Analysis of Buildings

By Erol Kalkan, M.ASCE^{1*} and Neal S. Kwong²

¹Research Structural Engineer, U.S. Geological Survey, Menlo Park, CA 94025, ekalkan@usgs.gov

² Ph.D. Candidate, University of California, Berkeley, CA 94709, nealsimonkwong@berkeley.edu

Abstract

According to the regulatory building codes in U.S. (e.g., 2010 California Building Code), at least two horizontal ground motion components are required for three-dimensional (3D) response history analysis (RHA) of buildings. For sites within 5 km of an active fault, these records should be rotated to fault-normal/fault-parallel (FN/FP) directions, and two RHA analyses should be performed separately (when FN and then FP are aligned with transverse direction of the structural axes). It is assumed that this approach will lead to two sets of responses that envelope the range of possible responses over all non-redundant rotation angles. This assumption is examined here, for the first time, using a 3D computer model of a six-story reinforced-concrete instrumented building subjected to an ensemble of bi-directional near-fault ground motions. Peak responses of engineering demand parameters (EDPs) were obtained for rotation angles ranging from 0° through 180° for evaluating the FN/FP directions. It is demonstrated that rotating ground motions to FN/FP directions (1) does not always lead to the maximum responses over all angles, (2) does not always envelope the range of possible responses, and (3) does not provide maximum responses for all EDPs simultaneously even if it provides a maximum response for a specific EDP.

Introduction

In U.S., both the California Building Code (ICBO, 2010) and International Building Code (ICBO, 2009) refer to ASCE/SEI-7 Chapter-16 (ASCE, 2010) when RHA is required for design verification of building structures. For three-dimensional (3D) analyses of symmetric-plan buildings, ASCE/SEI-7 requires either spectrally matched or intensity-based scaled ground motion records, which consist of pairs of appropriate

*Corresponding author

27 horizontal ground acceleration components. For each pair of horizontal components, a square root of the
28 sum of the squares (SRSS) spectrum shall be constructed by taking the SRSS of the 5% damped response
29 spectra of the unscaled components. Each pair of motions shall then be scaled with the same scale factor
30 such that the mean of the SRSS spectra does not fall below the corresponding ordinate of the target
31 spectrum in the period range from $0.2T_1$ to $1.5T_1$ (where T_1 is the elastic first-“mode” vibration period of the
32 structure). The design value of an engineering demand parameter (EDP)—member forces, member
33 deformations or story drifts—shall then be taken as the mean value of the EDP over seven (or more)
34 ground motion pairs, or its maximum value over all ground motion pairs, if the system is analyzed for fewer
35 than seven ground motion pairs. This procedure requires a minimum of three records.

36 As input for RHAs, strong motion networks provide users with ground accelerations recorded in three
37 orthogonal directions—two horizontal and one vertical. The sensors recording horizontal accelerations are
38 often, but not always, oriented in the North-South (N-S) and East-West (E-W) directions. These records
39 with station-specific orientations are referred to as “as-recorded” ground motions. If the recording
40 instrument had been installed in a different orientation about the vertical axis than the N-S and E-W
41 directions, and the corresponding pair of ground motions was of interest, then a two-dimensional rotation
42 transformation can be applied to the as-recorded motion. Since the instrument could have been installed at
43 any angle, the rotated versions are possible realizations.

44 Although the as-recorded pair of ground motion may be applied to the structural axes corresponding to
45 the structure’s transverse and longitudinal directions, there is no reason why the pair should not be
46 applied to any other axes rotated about the structural vertical axis. Equivalently, there is no reason why
47 rotated versions should not be applied to the structural axes. Which angle, then, should one select for RHA
48 remains a question in earthquake engineering practice.

49 This notion of rotating ground motion pairs has been studied previously in various contexts. According
50 to Penzien and Watabe (1975), the principal axis of a pair of ground motions is the angle or axis at which
51 the two horizontal components are uncorrelated. Using this idea of principal axis, the effects of seismic
52 rotation angle, defined as the angle between the principal axes of the ground motion pair and the structural
53 axes, on structural response was investigated (Franklin and Volker, 1982; Fernandez-Davilla et al., 2000;
54 MacRae and Matteis, 2000; Tezcan and Alhan, 2001; Khoshnoudian and Poursha, 2004; Rigato and
55 Medina, 2007). A formula for deriving the angle that yields the peak elastic response over all possible non-
56 redundant angles, called θ_{critical} (or θ_{cr}), was proposed by Wilson (1995). Other researchers have improved

57 upon the closed-form solution of Wilson (1995) by accounting for the statistical correlation of horizontal
58 components of ground motion in an explicit way (Lopez and Tores, 1997; Lopez et al., 2000). The Wilson
59 (1995) formula is, however, based on concepts from response spectrum analysis – an approximate
60 procedure used to estimate structural responses in the linear-elastic domain. Focusing on linear-elastic
61 multi-degree-of-freedom symmetric and asymmetric structures, Athanatopoulou (2005) investigated the
62 effect of the rotation angle on structural response using RHAs, and provided formulas for determining the
63 maximum response over all rotation angles, given the response histories for two orthogonal orientations.
64 Athanatopoulou (2005) also concluded that the critical angle corresponding to peak response over all
65 angles varies not only with the ground motion pair under consideration, but with the response quantity of
66 interest as well.

67 According to the Section 1615A.1.25 of the California Building Code (ICBO, 2010), at sites within 3
68 miles (5 km) of the active fault that dominates the hazard, each pair of ground motion components shall be
69 rotated to the fault-normal and fault-parallel (FN/FP) directions (also called as strike-normal and strike-
70 parallel directions) for 3D RHAs. It is believed that the angle corresponding to the FN/FP directions will lead
71 to the most critical structural response. This assumption is based on the fact that, in the proximity of an
72 active fault system, ground motions are significantly affected by the faulting mechanism, direction of rupture
73 propagation relative to the site, as well as the possible static deformation of the ground surface associated
74 with fling-step effects (Kalkan and Kunnath, 2006); these near-source effects cause most of the seismic
75 energy from the rupture to arrive in a single coherent long-period pulse of motion in the FN/FP directions
76 (Kalkan and Kunnath, 2007; 2008). Thus, rotating ground motion pairs to FN/FP directions is assumed to
77 be a conservative approach appropriate for design verification of new structures or performance evaluation
78 of existing structures.

79 Using a 3D structural model of an instrumented building and an ensemble of near-fault ground motion
80 records, this study systematically evaluates whether FN/FP directions rotated ground motions lead to
81 conservative estimates of EDPs from RHAs.

82 **Description of Structural System and Computer Model**

83 The testbed system used is a 3D computer model of the former Imperial County Services building in El
84 Centro, California. This relatively symmetrical building had an open first story and five occupied stories (Fig.
85 1). Designed in 1968, its vertical load carrying system consisted of 12.7 cm reinforced-concrete (RC) thick

86 slabs supported by RC pan joists, which in turn are supported by RC frames spanning in the orthogonal
87 direction. Figure 2 shows the foundation and typical floor layouts. Lateral resistance of all levels in the
88 longitudinal (E-W) direction was provided by two exterior moment frames at column lines 1 and 4, and two
89 interior moment frames on column lines 2 and 3. The lateral resistance in the transverse (N-S) direction
90 was not continuous. At the ground floor level, it was provided by four short shear walls located along
91 column lines A, C, D, and E and extending between column lines 2 and 3 only (Fig. 2 top). At the second
92 floor and above, lateral (N-S) resistance was provided by two shear walls at the east and west ends of the
93 building. This caused the building to be top heavy with a soft first story as shown in Figure 1 (Todorovska
94 and Trifunac, 2008). The design strength of the concrete was 34.5 MPa for columns, 20.7 MPa for the
95 elements below ground level, and 27.6 MPa elsewhere. All reinforcing steel was specified to be grade 40
96 ($F_y = 276$ MPa). The foundation system consisted of piles under each column with pile caps connected with
97 RC beams (Fig. 2 top).

98 The building was instrumented in 1976 with 13 sensors at four levels of the building and 3 sensors at a
99 reference free-field site. The sensors in the building measure horizontal accelerations at the ground floor,
100 2nd floor, 4th floor and roof; vertical acceleration was measured at the ground floor; the instrumentation lay
101 out of the building is given in Kalkan and Kwong (2012). The recorded motions of this building are available
102 only for the Mw 6.5 1979 Imperial Valley earthquake, during which this building was damaged and
103 subsequently demolished. The peak recorded accelerations during this earthquake were 0.34 g at the
104 ground floor and 0.58 g at the roof level. This building is a rare case of an instrumented building severely
105 damaged by an earthquake (Goel and Chadwell, 2007). Figure 1 (bottom) shows the concentration of
106 damage in the ground floor columns as a result of concrete spalling and buckling of reinforcing bars. The
107 details about the design, recorded data and observed damage can be found in Kojic et al. (1984).

108 The 3D computer model of this building was created using OpenSees (2010). Centerline dimensions
109 were used in the element modeling, the composite action of floor slabs was not considered, and the
110 columns were assumed to be fixed at the base level. For the response history evaluations, masses were
111 applied to frame models based on the floor tributary area, and distributed proportionally to the floor nodes.
112 The simulation models were calibrated to the response data measured during the Imperial Valley
113 Earthquake so as to validate and verify the analytical results of the comparative study.

114 Table 1 lists the linear-elastic periods of the first several modes, along with their modal participation
115 and contribution factors (Chopra, 2007) for two orthogonal directions along the structural axes. The

116 fundamental mode is primarily along the moment-frame (E-W direction) or X-direction of the computer
 117 model. As shown in Table 1, the period of the structure along this direction is 1.2 s, while the period of the
 118 structure in the Y-direction is 0.4 s, which is the period of the second mode. The irregularities in the N-S
 119 stiffness at the ground floor appear to have resulted in excessive torsional response and in significant
 120 coupling of the N-S and torsional excitations and responses. For the (N-S direction) or Y-direction, the
 121 structure is not “first-mode dominated” as the modal contribution factor for the first mode in this direction is
 122 only 68%.

123 **Ground-Motions Selected**

124 For this investigation, twenty near-fault strong motion records, listed in Table 2, were selected from ten
 125 shallow crustal earthquakes compatible with the following scenario:

- 126 • Moment magnitude: $M_w=6.7\pm 0.2$
- 127 • Closest-fault distance: $0.1\leq R_{rup}\leq 11$ km
- 128 • NEHRP soil type: C or D

129 Shown in Figure 3 are the 5% damped response spectra for the X- and Y-component of the as-
 130 recorded ground-motions. Also shown is the median spectrum, computed as the geometric mean of twenty
 131 response spectra in each direction. The median spectra show significantly large demands at the first and
 132 second mode of the building in both directions.

133 **Methodology for Evaluation of Fault-Normal/Parallel Directions**

134 Restricting ourselves to the linear-elastic version of the structural model, we invoke the principle of
 135 superposition when computing structural responses for a range of angles. The effective earthquake force in
 136 the governing equations of motion for excitation in the as-recorded direction and that for its orthogonal
 137 counterpart are, respectively:

$$\begin{aligned}
 \mathbf{p}_{eff}^{(1)} &= -\mathbf{M}[\mathbf{i}_x\ddot{u}_{gx} + \mathbf{i}_y\ddot{u}_{gy}] \\
 \mathbf{p}_{eff}^{(2)} &= -\mathbf{M}[-\mathbf{i}_x\ddot{u}_{gy} + \mathbf{i}_y\ddot{u}_{gx}]
 \end{aligned}
 \tag{1}$$

139 where the second load case is obtained by transforming the original as-recorded ground motion pair by a
 140 clockwise 90° rotation. For an arbitrary direction, the effective earthquake force can be written as:

$$\begin{aligned}
\mathbf{p}_{eff}^{(arb)} &= -\mathbf{M}[\mathbf{i}_x \ddot{u}_{gx}^{arb} + \mathbf{i}_y \ddot{u}_{gy}^{arb}] \\
&= -\mathbf{M}[\mathbf{i}_x \{\cos \theta \ddot{u}_{gx} - \sin \theta \ddot{u}_{gy}\} + \mathbf{i}_y \{\sin \theta \ddot{u}_{gx} + \cos \theta \ddot{u}_{gy}\}] \\
&= -\mathbf{M}[\cos \theta \{\mathbf{i}_x \ddot{u}_{gx} + \mathbf{i}_y \ddot{u}_{gy}\} + \sin \theta \{-\mathbf{i}_x \ddot{u}_{gy} + \mathbf{i}_y \ddot{u}_{gx}\}]
\end{aligned} \tag{2}$$

As a result, under the linear-elastic domain, the response histories for any arbitrary angle may be computed as a linear combination of two sets of response histories – one corresponding to the as-recorded orientation and the other corresponding to its orthogonal counterpart as:

$$\mathbf{r}^{(arb)} = \cos \theta \mathbf{r}^{(1)} + \sin \theta \mathbf{r}^{(2)} \tag{3}$$

where $\mathbf{r}^{(arb)}$ is the response history for any arbitrary angle, and $\mathbf{r}^{(1)}$ and $\mathbf{r}^{(2)}$ are the two sets of response histories.

Viewing the response as both a function of time and rotation angle enables us to better understand how the critical angle θ_{cr} , defined as the angle corresponding to the largest response over all non-redundant rotation angles, varies with both EDP and ground motion pair. For a given response quantity of interest and record pair, the FN/FP directions will correspond to two values (i.e., FN and FP rotated ground motions are applied along X- and Y-axis, then along Y- and X-axis). By comparing these two values with the responses at all other possible angles, one can evaluate the level of conservatism in such directions. If obvious systematic benefits of the FN/FP orientations existed, they should be observable by repeating such comparisons for several EDPs and record pairs.

Even if no obvious trends are observed, one can still compare the FN/FP directions with the no rotation case at all. Rather than comparing the FN/FP directions to the as-recorded directions, however, the as-recorded direction may be viewed as an arbitrarily assigned orientation. As a result, one will be able to state the *likelihood* of the FN/FP responses being conservative instead of simply stating whether or not it was conservative.

If the rotation angle θ for a record pair was the only source of uncertainty and the probability distribution for θ was specified, then a conditional probability density function (PDF) for the structural response may be defined. In particular, if θ is uniformly distributed from 0° through 180° , then the PDF for the EDP may be estimated by (1) obtaining a random sample of n rotation angles based on the uniform distribution, (2) computing the EDP corresponding to each of the n angles, and (3) forming a histogram with the collection of EDP values (Wasserman, 2004). Equipped with an estimate of the EDP's probability distribution, conditioned on a ground motion pair, one can approximately determine the probability of

168 exceeding the FN/FP responses. Low probabilities of exceedance would suggest that there is some merit in
169 focusing our attention to the FN/FP directions.

170 **Structural Response Variability with Rotation Angle**

171 According to the ASCE/SEI-7 provisions under Section 16.1.3.2, the horizontal components are to be
172 identically scaled such that the average of the SRSS spectra from all scaled horizontal component pairs
173 exceed the target design spectrum (defined under ASCE/SEI-7 Section 11.4.5 or 11.4.7) over the period
174 range of $0.2T_1$ to $1.5T_1$.

175 *How will the SRSS spectrum change if the ground motion pair was rotated?*

176 By rotating each of the twenty record pairs in Table 2 from 0° to 180° with a 5° interval clock-wise, one
177 can compute 37 alternative SRSS spectra. Figure 4 shows the maximum and minimum envelopes
178 bounding such rotated versions of the SRSS response spectra for each ground motion pairs (no scaling is
179 applied). In this figure, D_{rms} refers to root mean square, a metric used to quantify the variability of spectral
180 accelerations (S_a) with changing rotation angle. D_{rms} is computed for each rotation angle over all spectral
181 periods as:

$$182 \quad D_{rms} = \sqrt{\frac{1}{N} \sum_{i=1}^N [\ln(Sa_{max,i}) - \ln(Sa_{min,i})]^2} \quad (4)$$

183 where i refers to the i^{th} spectral period and N is the total number of logarithmically spaced spectral periods.
184 It is visually evident that the SRSS response spectrum vary marginally with rotation angle. The relatively
185 small D_{rms} values indicate that several rotated versions of the ground motion pair can satisfy the ASCE
186 criteria and yet provide structural responses that are different (as shown later). This figure also implies that
187 rotating ground motions has a marginal effect on the ground motion scaling factors computed for each pair
188 to satisfy the ASCE criteria.

189 *How much variability is there in the elastic structural responses as the rotation angle is varied?*

190 Figure 5 addresses this question by showing the drifts in the longitudinal (E-W or X) direction for the
191 first story as a function of the rotation angle for all records. To better understand the relative variability,
192 each subplot was normalized by the maximum response over all angles. Maximum responses for individual
193 ground motion pairs were found to occur at different angles. With the exception of a few pairs, the first story

194 drift (i.e., inter-story drift) in X-direction can vary by a factor of 2 over the possible angles of interest. This is
195 considered to be a large variation.

196 Although this figure indicates that the first story drift in X-direction does not vary significantly with
197 rotation angle for ground motion pair number three, the same statement cannot be made for other response
198 quantities. Considering pair number three, various other response quantities are shown as a function of
199 rotation angle in Figure 6. It is evident that peak values of other EDPs occur at different angles for the same
200 record pair. Large variation for EDPs other than story drift is also observed. For example, the torsion for an
201 arbitrarily selected column can vary by a factor of 2 over the possible angles.

202 To better quantify this variation with rotation angle, the coefficient of variation (COV) is computed using
203 equation 5 for each ground motion pair and for each response quantity related to an arbitrarily selected
204 corner column in the first story. These values are shown in Table 3.

$$205 \quad COV = \frac{\sqrt{\frac{1}{n-1} \sum_{i=1}^n (x_i - \bar{x})^2}}{\bar{x}} \quad (5)$$

206 The COV for M_x is larger for pair number one than for pair number two. The reverse is true, however, when
207 the response quantity of interest is M_y instead. Here, the COV is larger for the second pair than for the first
208 pair. These results demonstrate that one must consider *both* the response quantity of interest and the
209 ground motion characteristics when attempting to predict the variability with respect to rotation angle in
210 advance.

211 The fact that the variability depends on both the response quantity and ground motion pair can also be
212 observed in Figure 7, where the height-wise distribution of story drifts in X-direction over several angles is
213 shown. In order to illustrate the variability in the responses within each pair, a common scale was not used
214 for the drift axis. The variability is significantly large for some ground motion pairs (for example, pair no. 12,
215 15 and 18), as compared to smaller variability observed for pair no. 3, 16, 17. For the 5th pair of ground
216 motion, the drift in the second story varies much more than the drift in the sixth story, indicating that higher-
217 mode effects, contributing to the response with larger demands at upper stories, become more pronounced
218 at certain angles only. Similar results for the Y-direction are shown in Kalkan and Kwong (2012). These
219 results also confirm the fact that θ_{cr} varies with ground motion and with response quantity of interest. This is
220 because θ_{cr} is a quantity that is highly dependent on the complete response history of the EDP. As a result,
221 determining a rotation angle that yields a conservative estimate of structural response simultaneously for

222 both a large number of response quantities (EDPs) and ground motion records is difficult, it is easy,
223 however, to compute θ_{cr} for a single EDP under a single pair of accelerograms (Athanatopoulou, 2005).

224 **Evaluation of Fault-Normal/Parallel Directions Rotated Ground Motions**

225 In order to evaluate the usefulness of rotating a record pair to the FN/FP directions, a practice commonly
226 exercised, the EDPs corresponding to the FN/FP directions are compared against those corresponding to
227 all other directions. To limit the computations to a reasonable size, each as-recorded pair is rotated clock-
228 wise by increments of 10° instead of 5° before the EDPs are calculated. As a result, the two FN/FP sets of
229 responses are compared against 19 other sets.

230 For example, the 21 height-wise distributions of story drifts in the X-direction, for each record pair, are
231 shown in Figure 8; plots showing drifts in the Y-direction are shown in Kalkan and Kwong (2012). The
232 distribution of drifts corresponding to the FN direction is highlighted in red, while that corresponding to the
233 FP direction is highlighted in green. In order to display the variability in responses within each pair, the drift
234 values are normalized by the maximum drift value over all 19 angles and over the entire height. For some
235 pairs (for example, pair no. 5, 6 and 8), the maximum of the FN/FP drifts is NOT the largest among all
236 possibilities. Visually, the maximum of the FN/FP drifts is the largest among all possibilities approximately
237 only for 10 of the 20 record pairs. Consequently, the FN/FP drifts are NOT always conservative.

238 Whether or not the FN/FP drifts are conservative depends not only on the ground motion pair but also
239 on the EDP. For instance, although the FN direction yields the maximum height-wise distribution of drifts in
240 the X-direction for pair no. 18, the FN direction yields the minimum height-wise distribution of drifts in the Y-
241 direction for the same pair, as demonstrated in Figure 9. As another example, although the FP direction
242 yields the largest roof drift in the X-direction for pair no. 5, the same direction for the same pair does not
243 guarantee a conservative first story drift in the X-direction, as demonstrated in Figure 8. Thus, one cannot
244 be certain that the worst-case responses are always obtained when performing RHAs with ground motions
245 rotated to the FN/FP directions.

246 *If the FN/FP directions do not generate the maximum responses for all response quantities and for all*
247 *ground motion pairs, is there still a merit to rotate an as-recorded pair prior to performing response history*
248 *analyses?*

249 To address this issue, the FN/FP directions rotated ground motions are evaluated from a statistical
250 viewpoint. Suppose the only source of aleatoric uncertainty in responses is due to uncertainty in the

251 rotation angle of the ground motion pair. In other words, given the structural model and ground motion pair,
252 the EDP will have a probability distribution that is directly related to the probability distribution for the
253 rotation angle. This conditional distribution for the EDP can serve as a benchmark to evaluate the
254 usefulness in rotating as-recorded ground motions to the FN/FP directions.

255 Because the functional relationship between the EDP and the rotation angle is different for each EDP
256 of interest, the conditional probability distribution will be different for different EDPs. Moreover, because the
257 functional relationship is generally complex (especially for nonlinear-inelastic systems), direct analytical
258 determination of the probability distribution is not feasible. Consequently, Monte Carlo simulation is used
259 here to estimate these distributions. Assuming the rotation angle is a uniformly distributed random variable,
260 a random sample of angles is generated. For each angle in the random sample, the EDP of interest is
261 determined. Summarizing such data in the form of histograms, for all record pairs and for the first story drift
262 in the X-direction, leads to plots shown in Figure 10; similar plots for Y-direction are shown in Kalkan and
263 Kwong (2012).

264 The histograms in this figure may be interpreted as approximate probability density functions (PDFs)
265 for the normalized EDPs (normalized by their maximum values). The normalized scales confirm that the
266 response variability depends on both the record pair and the EDP of interest. These approximate densities
267 are bounded since the range of possible rotation angles is finite. A majority of the approximate PDFs share
268 a common shape. Specifically, the distributions appear to be bi-modal, with the modal values often at the
269 extremes, also valid for other EDPs. A rough interpretation of this is that if one were to determine the EDP
270 corresponding to a randomly chosen angle, the EDP would most likely be a maximum or a minimum value
271 (rather than somewhere in between) with respect to all possible values. If one were to take the EDP as the
272 larger of the FN/FP EDPs instead, Figure 10 illustrates that the value would be usually larger than half of all
273 possible responses.

274 To quantify the latter observations, the concept of cumulative distribution functions (CDF*) is utilized.
275 Approximate CDFs for the normalized first story drifts in X-direction are shown in Figure 11 (similar plots
276 are shown for Y-direction in Kalkan and Kwong, 2012). This figure is simply the data from Figure 10 re-
277 plotted in a different way. The steep slope near the ends of the CDFs is consistent with the previous
278 observation that responses near the extremes of the possible range have higher probabilities of occurring
279 relative to other values. To understand what information the larger (blue) of the FN (red) and FP (green)

* CDF of x , or $F(x)$, indicates the probability of observing a value equal to or less than the value of x .

280 responses provides, we will focus on the first subplot in Figure 11. The subplot indicates that there is
 281 approximately a 65% probability of observing a first story drift value less than or equal to the FP value
 282 identified in blue (in this case it is also the larger of the FN/FP values). Equivalently, there is approximately
 283 a 35% probability of the FP value underestimating the drift for precisely record pair no. 1. Focusing on the
 284 blue lines for all record pairs next, one observes that the probability of observing a drift value larger than
 285 the maximum of the FN/FP value is consistently less than 50% for all record pairs. However, this trend is
 286 not perfect, as demonstrated for pair no. 8 and 13 for the Y-direction drifts in Kalkan and Kwong (2012).

287 The CDFs, and the associated probability statements, are approximate because the empirical
 288 cumulative distribution functions (ECDFs) were shown instead of the true CDFs. In probability and
 289 statistics, the ECDF is an estimate of the CDF obtained using a random sample from the true CDF
 290 (Wasserman 2004). Assigning an equal probability to each value in the random sample of size n and using
 291 equation 6 leads to a staircase curve known as the ECDF

$$292 \quad \hat{F}_n(t) = \frac{1}{n} \sum_{i=1}^n 1\{X_i \leq t\} \quad (6)$$

293 where X_i is the i^{th} value in the random sample of size n and 1 is the indicator function – it is 1 only if the
 294 event in the brackets is true and 0 otherwise. As the sample size increases, the ECDF converges almost
 295 surely to the true CDF because of the Glivenko-Cantelli theorem (Dudley, 1999). This is shown in Kalkan
 296 and Kwong (2012) when 100, 1,000, and 5,000 different random samples of the first story drift in X-
 297 direction are used to compute the ECDF. The curve corresponding to the use of 1,000 values is virtually
 298 indistinguishable from that associated with the use of 5,000 values. As a result, 1,000 values were used to
 299 construct the histograms and ECDFs in the previous figure.

300 Since the conditional ECDFs vary depending on response quantity, the benchmark evaluations of the
 301 FN/FP directions should be performed considering several response quantities. Using a sample size of
 302 5,000, Table 4 shows the probabilities of exceeding the larger of the FN/FP responses for story drifts in all
 303 stories and in both orthogonal directions of the structure. These probabilities of exceedance may be
 304 interpreted as the amount of error one makes in deciding to use the larger of the FN/FP response as the
 305 “worst-case” value among all possibilities. Considering errors from round-off and the use of a finite random
 306 sample, Table 4 numerically confirms that there is always some probability of obtaining a response value
 307 larger than that associated with the FN and FP directions. In other words, there is always some amount of
 308 error made when deciding to use the FN/FP response as the “worst” among all angles. However, the cells

309 with probabilities smaller than 15% (highlighted in green) may be viewed as instances where the FN/FP
310 value is essentially conservative (15% is a widely accepted threshold for safety for engineering
311 applications). It is numerically confirmed in Table 4 that such conservatism typically varies with response
312 quantities and record pair.

313 With such numerical results, one can address whether rotation to the FN/FP directions is worthwhile.
314 One alternative to deliberate rotation is to utilize the as-recorded orientation, which can be viewed as a
315 randomly selected direction. The response from such an arbitrary orientation may be larger or smaller than
316 the FN/FP values.

317 *How often does the value of response quantity from the arbitrary-direction exceed that of the FN/FP*
318 *value?*

319 The probability values presented in Table 4 provide the answer. For example, the 35% value for record
320 pair no. 1 and first story drift in X-direction means that, among 5,000 trials, the response corresponding to a
321 randomly chosen direction exceeds the FN/FP value 35% of the time. However, the latter remark is not
322 valid for ALL record pairs and ALL response quantities, as demonstrated by the cells highlighted in red in
323 Table 4. For instance, the 72% value for record pair no. 13 and first story drift in Y-direction means that the
324 response corresponding to a randomly chosen direction exceeds the FN/FP value 72% of the time. Thus,
325 the FN/FP directions are less conservative in this particular case. Nevertheless, the relatively few red cells
326 suggests that using the larger of the FN/FP response typically, BUT NOT ALWAYS, leads to a value larger
327 than that from a randomly chosen/as-recorded direction.

328 **Conclusions**

329 The current state-of-practice in U.S. is to rotate the as-recorded pair of ground motions to the fault-normal
330 and fault-parallel (FN/FP) directions before they are used as input for three-dimensional response history
331 analyses (RHAs) of structures within 5 km of active fault(s). It is assumed that this approach will lead to two
332 sets of responses that envelope the range of possible responses over all non-redundant angles of rotation.
333 Thus, it is considered to be a conservative approach appropriate for design verification of new structures.
334 Based on a linear-elastic computer model of a six-story instrumented structure, this study, for the first time,
335 evaluates the relevance of using the FN/FP directions in RHAs, and demonstrates its pros and cons in the
336 following:

- 337 1. It was shown that rotated versions of the square-root-of-sum-of-squares (SRSS) response spectra
338 following the ASCE/SEI-7 provisions under Section 16.1.3.2, does not vary much with rotation
339 angle—the maximum difference observed is less than 10%. Several rotated versions of the ground
340 motion pair can satisfy the ASCE criteria and yet provide structural responses that can vary by a
341 factor of 2.
- 342 2. The critical angle θ_{cr} corresponding to the largest response over all possible angles varies with the
343 ground motion pair selected and the response quantity of interest. Therefore, it is difficult to
344 determine an “optimal” building orientation that maximizes demands for all EDPs before response
345 history analyses are conducted.
- 346 3. The use of the FN/FP directions applied along the principal directions of the building almost never
347 guarantees that the maximum response over all possible angles will be obtained. Even though it
348 may lead to a maximum for a specific EDP, it will simultaneously be unconservative for other
349 EDPs. Therefore, if the performance assessment and design verification will be conducted against
350 the worst-case scenarios, then bi-directional ground motions should be applied at various angles
351 with respect to the structure’s principal directions to cover all possible responses. Although this
352 might not be a practical solution, it could still be worth conducting for certain projects.
- 353 4. Treating the as-recorded direction as a randomly chosen direction, it is observed that there is more
354 than a 50% probability for the larger response among the FN and FP values to exceed the
355 response corresponding to an arbitrary orientation. The latter observation is valid for most, BUT
356 NOT ALL, of the record pairs and response quantities considered. Therefore, compared to no
357 rotation at all, use of the larger response among the two values corresponding to the FN and FP
358 directions is warranted.

359 Although these observations and findings are primarily applicable to buildings and ground motions with
360 characteristics similar to those utilized in this study, they are in close agreement with those reported in
361 Reyes and Kalkan (2012a,b), where the influence of rotation angle on several EDPs has been examined in
362 a parametric study using symmetric (torsionally-stiff) and asymmetric (torsionally-flexible) modern design
363 single-story and multi-story linear-elastic and nonlinear-inelastic buildings subjected to a different set of
364 near-fault records.

365 **Acknowledgments**

366 Neal S. Kwong would like to acknowledge the U.S. Geological Survey for providing him the financial
367 support for conducting this research. Special thanks are extended to Rakesh Goel for generously providing
368 the OpenSees model of the Imperial County Services building. Rui Chen, Alex Taflanidis, Dimitrios
369 Vamvatsikos, Aysegul Askan, Ricardo Medina, and three anonymous reviewers have reviewed the material
370 presented herein, and offered their valuable comments and suggestions, which helped improving the
371 technical quality and presentation of this paper.

372 **References**

- 373 ASCE, 2010, Minimum design loads for buildings and other structures, ASCE/SEI 7-10, Reston, VA.
- 374 Athanatopoulou, A.M., 2005, Critical orientation of three correlated seismic components, *Engineering*
375 *Structures*, v.27, n.1, p.301-312.
- 376 Dudley, R.M., 1999, Uniform Central Limit Theorems, Cambridge University Press.
- 377 Fernandez-Davila, I., Comeinetti, S. and Cruz, E.F., 2000, Considering the bi-directional effects and the
378 seismic angle variations in building design, *Proc. of the 12th World Conference on Earthquake*
379 *Engineering*.
- 380 Franklin, C.Y. and Volker, J.A., 1982, Effect of various 3-D seismic input directions on inelastic building
381 systems based on INRESB-3D-82 Computer Program, *Proc. of the 7th European Conference on*
382 *Earthquake Engineering*.
- 383 Chopra, A. K., 2007, Dynamics of structures: Theory and applications to equation engineering, 2nd Ed.,
384 Prentice Hall: Englewood Cliffs, NJ.
- 385 Goel, R.K. and Chadwell, C., 2007, Evaluation of current nonlinear static procedures for concrete buildings
386 using recorded strong-motion data, CSMIP Data Interpretation Report, Sacramento, CA.
- 387 International Conference of Building Officials (ICBO), 2009, International Building Code, Whittier, CA.
- 388 International Conference of Building Officials (ICBO), 2010, California Building Code, Whittier, CA.
- 389 Kalkan, E. and Kunnath, S.K., 2006, Effects of Fling-Step and Forward Directivity on the Seismic Response
390 of Buildings, *Earthquake Spectra*, v.22, n.2, p.367-390.
- 391 Kalkan, E. and Kunnath, S.K., 2007, Effective Cyclic Energy as a Measure of Seismic Demand, *Journal of*
392 *Earthquake Engineering*, v.11, n.5, p.725-751.

393 Kalkan, E. and Kunnath, S.K., 2008, Relevance of Absolute and Relative Energy Content in Seismic
394 Evaluation of Structures, *Advances in Structural Engineering*, v.11, n.1, p.17-34.

395 Kalkan, E., and Kwong, N.S., 2012, Evaluation of fault-normal/fault-parallel directions rotated ground
396 motions for response history analysis of an instrumented six-story building: U.S. Geological Survey
397 Open-File Report 2012–1058, 30 p., available at <http://pubs.usgs.gov/of/2012/1058/>.

398 Khoshnoudian, F. and Poursha, M., 2004, Responses of three dimensional buildings under bi-directional
399 and unidirectional seismic excitations, *Proc. of the 13th World Conference on Earthquake Engineering*.

400 Kojic, S., Trifunac, M.D. and Anderson, J.C., 1984. A post earthquake response analysis of the Imperial
401 County Services Building in El Centro, Report CE 84-02, University of Southern California, Department
402 of Civil Engineering, Los Angeles, CA.

403 Lopez, O.A. and Torres, R., 1997, The critical angle of seismic incidence and structural response,
404 *Earthquake Engineering and Structural Dynamics*, v.26, p.881-894.

405 Lopez, O.A., Chopra, A.K. and Hernandez, J.J., 2000, Critical response of structures to multicomponent
406 earthquake excitation, *Earthquake Engineering and Structural Dynamics*, v.29, p.1759-1778.

407 MacRae, G.A. and Mattheis, J., 2000, Three-dimensional steel building response to near-fault motions,
408 *ASCE Journal of Structural Engineering*, v.126, n.1, p.117-126.

409 OpenSees 2010. Open system for earthquake engineering simulation. Available online at:
410 <http://opensees.berkeley.edu>.

411 Penzien, J. and Watabe, M., 1975, Characteristics of 3-Dimensional earthquake ground motions,
412 *Earthquake Engineering and Structural Dynamics*, v.3, p.365-373.

413 Reyes, J.C. and Kalkan, E., 2012a, Significance of the ground motion rotation angle on nonlinear behavior
414 of symmetric and asymmetric buildings in near fault sites, *Proc. of the 9th International Conf. on Urban
415 Earthquake Engineering / 4th Asia Conf. on Earthquake Engineering*, Tokyo, Japan (available online at
416 http://nsmg.wr.usgs.gov/ekalkan/PDFs/Conferences/C26_Reyes_Kalkan.pdf)

417 Reyes, J.C. and Kalkan, E., 2012b, Relevance of Fault-Normal/Parallel and Maximum Direction Rotated
418 Ground Motions on Nonlinear Behavior of Symmetric and Asymmetric Buildings: U.S. Geological
419 Survey Open-File Report 2012 (in-press).

420 Rigato, A., and Medina, R.A., 2007, Influence of Angle of Incidence on the Seismic Demands for Inelastic
421 Single-storey Structures Subjected to Bi-directional Ground Motions, *Engineering Structures*, v. 29,
422 n.10, p. 2593-2601.

423 Tezcan, S.S. and Alhan, C., 2001, Parametric analysis of irregular structures under seismic loading
 424 according to the new Turkish Earthquake Code, *Engineering Structures*, v. 23, p.600-609.

425 Todorovska, M.I. and Trifunac, M.D., 2008, Earthquake damage detection in the Imperial County Services
 426 Building III: analysis of wave travel times via impulse response functions, *Soil Dynamics and*
 427 *Earthquake Engineering*, v.28, n.5, p.387-404.

428 Wasserman, L., 2004, All of Statistics: A Concise Course in Statistical Inference. Springer: New York.

429 Wilson, E.L. and Suharwardy, I., 1995, A clarification of the orthogonal effects in a three-dimensional
 430 seismic analysis, *Earthquake Spectra*, v.11, n.4, p.659–666.

431

432

433 **Table 1. Linear-elastic dynamic properties of the Imperial County Services building: The modal participation**
 434 **(Γ) and modal contribution factors (MCF) are shown to illustrate how the first six modes contribute to the**
 435 **linear-elastic responses in two orthogonal directions.**

436

Mode Number (n)	Period (s)	$\Gamma_{n,x}$	$\Gamma_{n,y}$	MCF,x (%)	MCF,y (%)
1	1.2	5.3	0.0	84.5	0.0
2	0.4	0.0	4.8	0.0	68.4
3	0.4	-1.9	0.0	10.5	0.0
4	0.3	0.0	-0.8	0.0	1.9
5	0.2	-1.0	0.0	3.0	0.0
6	0.2	-0.7	0.0	1.4	0.0

437

438

Table 2. Selected near-fault strong ground-motion records

Pair No.	Earthquake Name	Year	Station Name	M_w	R_{rup} (km)	V_{S30} (m/s)	Fault-normal Component			Fault-parallel Component		
							PGA (g)	PGV (cm/s)	PGD (cm)	PGA (g)	PGV (cm/s)	PGD (cm)
1	Tabas, Iran	1978	Tabas	7.4	2.1	767	0.8	118	97	0.8	80	42
2	Imperial Valley, Calif.	1979	EC Meloland Overpass FF	6.5	0.1	186	0.4	115	40	0.3	27	15
3	Imperial Valley, Calif.	1979	El Centro Array #7	6.5	0.6	211	0.5	109	46	0.3	45	24
4	Superstition Hills, Calif.	1987	Parachute Test Site	6.5	1.0	349	0.4	107	51	0.3	50	22
5	Loma Prieta, Calif.	1989	Corralitos	6.9	3.9	462	0.5	45	14	0.5	42	7
6	Loma Prieta, Calif.	1989	LGPC	6.9	3.9	478	0.9	97	63	0.5	72	31
7	Erzincan, Turkey	1992	Erzincan	6.7	4.4	275	0.5	95	32	0.4	45	17
8	Northridge, Calif.	1994	Newhall - W Pico Canyon Rd	6.7	5.5	286	0.4	88	55	0.3	75	22
9	Northridge, Calif.	1994	Rinaldi Receiving Sta	6.7	6.5	282	0.9	167	29	0.4	63	21
10	Northridge, Calif.	1994	Sylmar - Converter Sta	6.7	5.4	251	0.6	130	54	0.8	93	53
11	Northridge, Calif.	1994	Sylmar - Converter Sta East	6.7	5.2	371	0.8	117	39	0.5	78	29
12	Northridge, Calif.	1994	Sylmar - Olive View Med FF	6.7	5.3	441	0.7	123	32	0.6	54	11
13	Kobe, Japan	1995	Takatori	6.9	1.5	256	0.7	170	45	0.6	63	23
14	Kocaeli, Turkey	1999	Yarimca	7.4	4.8	297	0.3	48	43	0.3	73	56
15	Chi-Chi, Taiwan	1999	TCU052	7.6	0.7	579	0.4	169	215	0.4	110	220
16	Chi-Chi, Taiwan	1999	TCU065	7.6	0.6	306	0.8	128	93	0.6	80	58
17	Chi-Chi, Taiwan	1999	TCU068	7.6	0.3	487	0.6	191	371	0.4	238	387
18	Chi-Chi, Taiwan	1999	TCU084	7.6	11.2	553	1.2	115	32	0.4	44	21
19	Chi-Chi, Taiwan	1999	TCU102	7.6	1.5	714	0.3	107	88	0.2	78	55
20	Duzce, Turkey	1999	Duzce	7.2	6.6	276	0.4	62	47	0.5	80	48

Table 3. Coefficient of variations (COV) for force (P) and moment (M or T) parameters along the X-, Y-, and Z-directions of a first-story corner column (X = longitudinal, Y = transverse, Z = vertical direction in plan view).

Pair No.	Coefficient of Variations for Arbitrary 1 st -story Corner Column					
	P _x (kips)	P _y (kips)	P _z (kips)	M _x (kip-in)	M _y (kip-in)	T _z (kip-in)
1	0.26	0.29	0.28	0.29	0.26	0.23
2	0.36	0.15	0.12	0.17	0.35	0.21
3	0.08	0.27	0.14	0.28	0.07	0.22
4	0.34	0.16	0.17	0.17	0.36	0.16
5	0.09	0.34	0.26	0.36	0.05	0.32
6	0.17	0.25	0.21	0.27	0.24	0.23
7	0.35	0.09	0.12	0.07	0.34	0.14
8	0.24	0.12	0.09	0.14	0.22	0.09
9	0.29	0.16	0.07	0.18	0.29	0.21
10	0.24	0.14	0.09	0.17	0.23	0.18
11	0.30	0.24	0.22	0.26	0.31	0.26
12	0.22	0.39	0.32	0.39	0.30	0.37
13	0.28	0.07	0.20	0.08	0.25	0.10
14	0.20	0.17	0.14	0.16	0.20	0.10
15	0.41	0.28	0.09	0.26	0.38	0.27
16	0.12	0.07	0.15	0.06	0.12	0.06
17	0.11	0.26	0.22	0.27	0.12	0.27
18	0.40	0.27	0.13	0.27	0.39	0.27
19	0.24	0.21	0.12	0.21	0.23	0.19
20	0.25	0.28	0.22	0.27	0.25	0.18

Table 4. Probabilities of exceeding the larger response among the FN/FP values for selected response quantities, estimated with 5,000 random samples. Story drifts for both orthogonal directions of the building are considered. Probabilities smaller than 15% are highlighted in green while probabilities larger than 50% are highlighted in red (DR_{x,n} means nth story drift in X-direction).

Pair No.	Probability of Exceeding Larger Response Among FN/FP Responses (in percent)											
	DR _{x,1}	DR _{x,2}	DR _{x,3}	DR _{x,4}	DR _{x,5}	DR _{x,6}	DR _{y,1}	DR _{y,2}	DR _{y,3}	DR _{y,4}	DR _{y,5}	DR _{y,6}
1	35	28	26	19	14	15	30	25	24	24	23	23
2	0	1	4	7	9	10	28	25	25	25	25	25
3	49	38	15	13	12	11	26	25	25	25	25	25
4	30	30	27	25	26	27	42	38	38	38	38	38
5	32	38	42	65	58	35	44	40	40	40	40	40
6	46	46	46	45	44	43	13	10	9	9	9	9
7	11	12	14	15	15	15	17	25	25	26	26	26
8	40	41	41	40	39	39	57	46	45	45	44	44
9	0	3	7	11	14	14	12	16	16	17	17	17
10	38	38	41	44	46	46	45	46	46	46	46	46
11	40	35	31	27	20	28	6	5	5	5	5	5
12	25	21	20	25	28	29	39	38	38	38	38	38
13	4	4	3	3	3	4	72	61	60	56	55	54
14	15	14	12	12	14	16	30	33	33	33	33	33
15	47	48	49	50	49	49	46	44	44	44	44	44
16	23	31	15	15	30	31	20	45	45	46	47	46
17	32	34	37	47	49	48	26	24	24	24	24	24
18	7	8	11	12	13	13	5	4	4	4	4	4
19	15	15	17	18	19	19	34	32	32	32	32	32
20	5	4	0	4	8	10	24	23	23	23	23	23



Figure 1. Imperial County Services building: (top) general view towards North, (bottom) damage of ground floor columns during the Mw 6.5 1979 Imperial Valley earthquake (modified with permission from Todorovska and Trifunac, 2008).

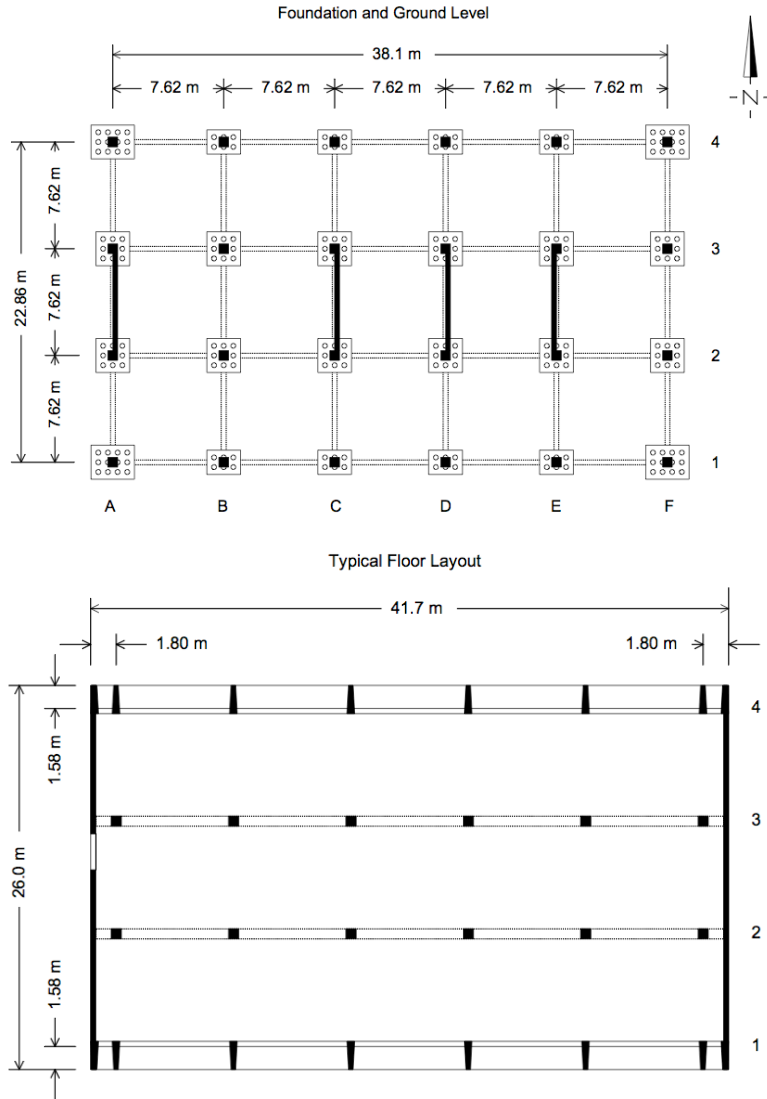


Figure 2. Foundation and ground level plan (top) and typical floor layout (bottom) of the Imperial County Services building (modified with permission from Todorovska and Trifunac, 2008).

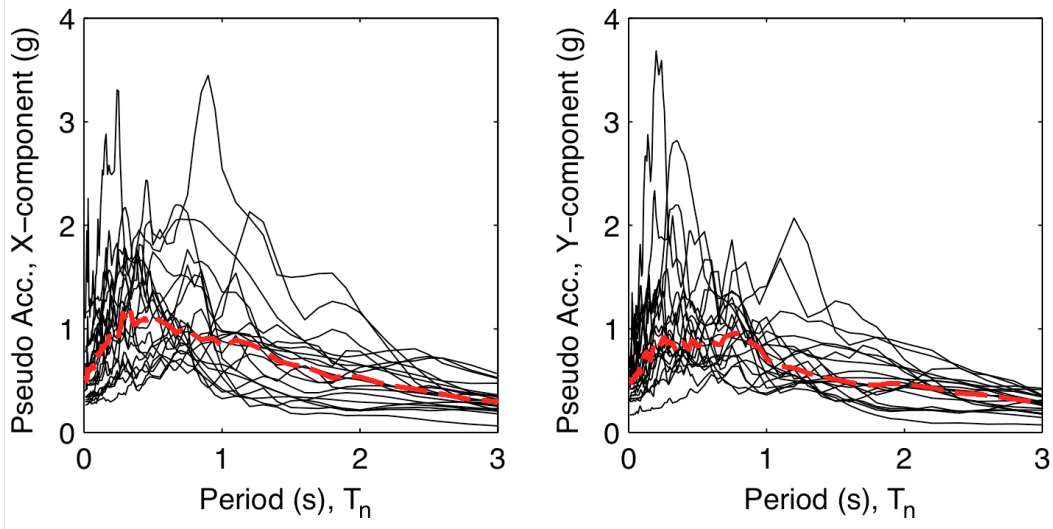


Figure 3. Pseudo acceleration response spectra of twenty near-fault strong ground-motions; damping ratio 5% (Red = median spectrum of all records).

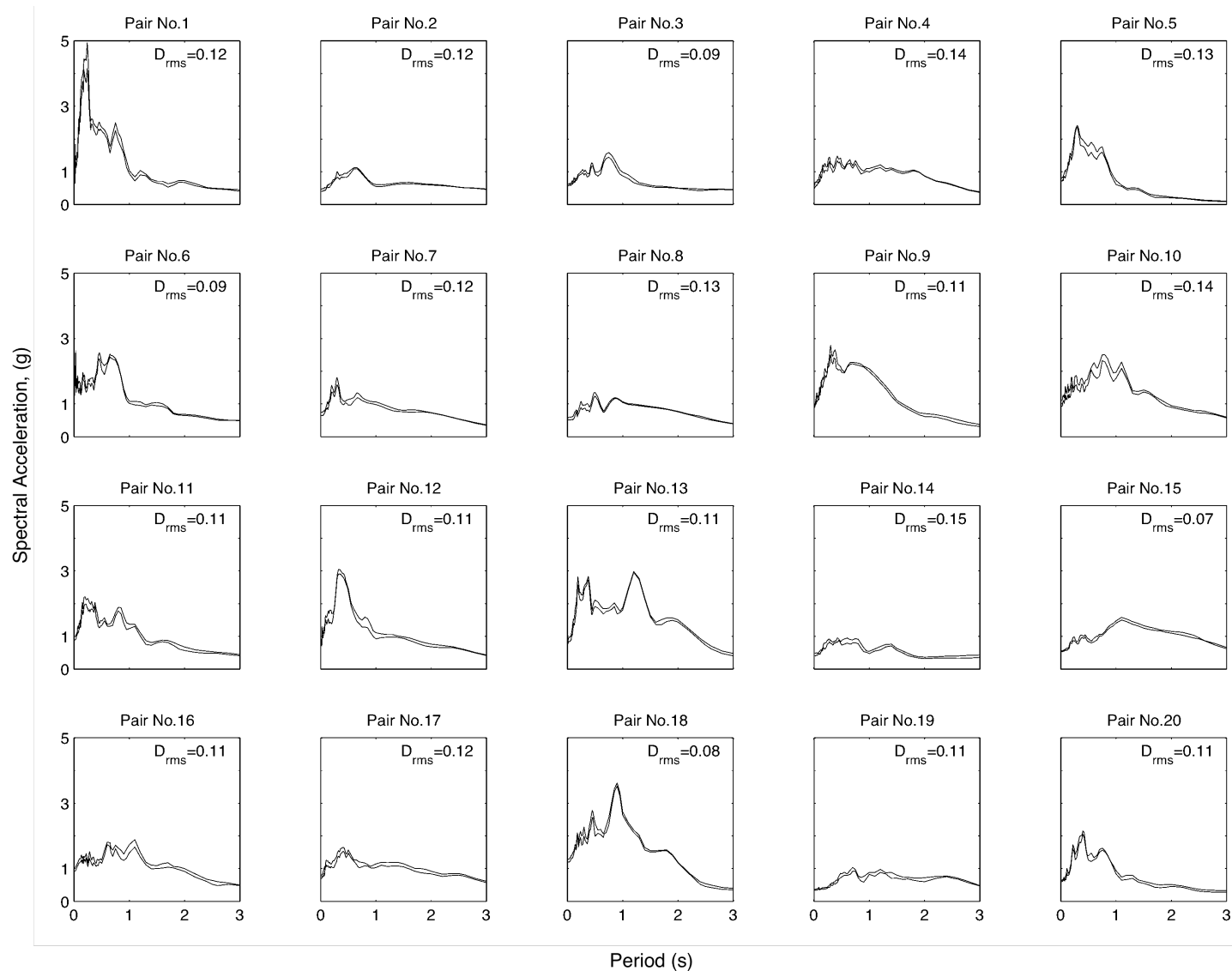


Figure 4. Maximum and minimum envelopes for square-root-of-sum-of-squares (SRSS) response spectra rotated through all angles from 0° through 180° with a 5° interval. The root-mean-square (D_{rms}) metric is shown for each horizontal pair of ground motion to indicate the degree of variation in rotated spectra; small values of D_{rms} in all panels indicate that variation of spectral values by rotating ground motion components is insignificant.

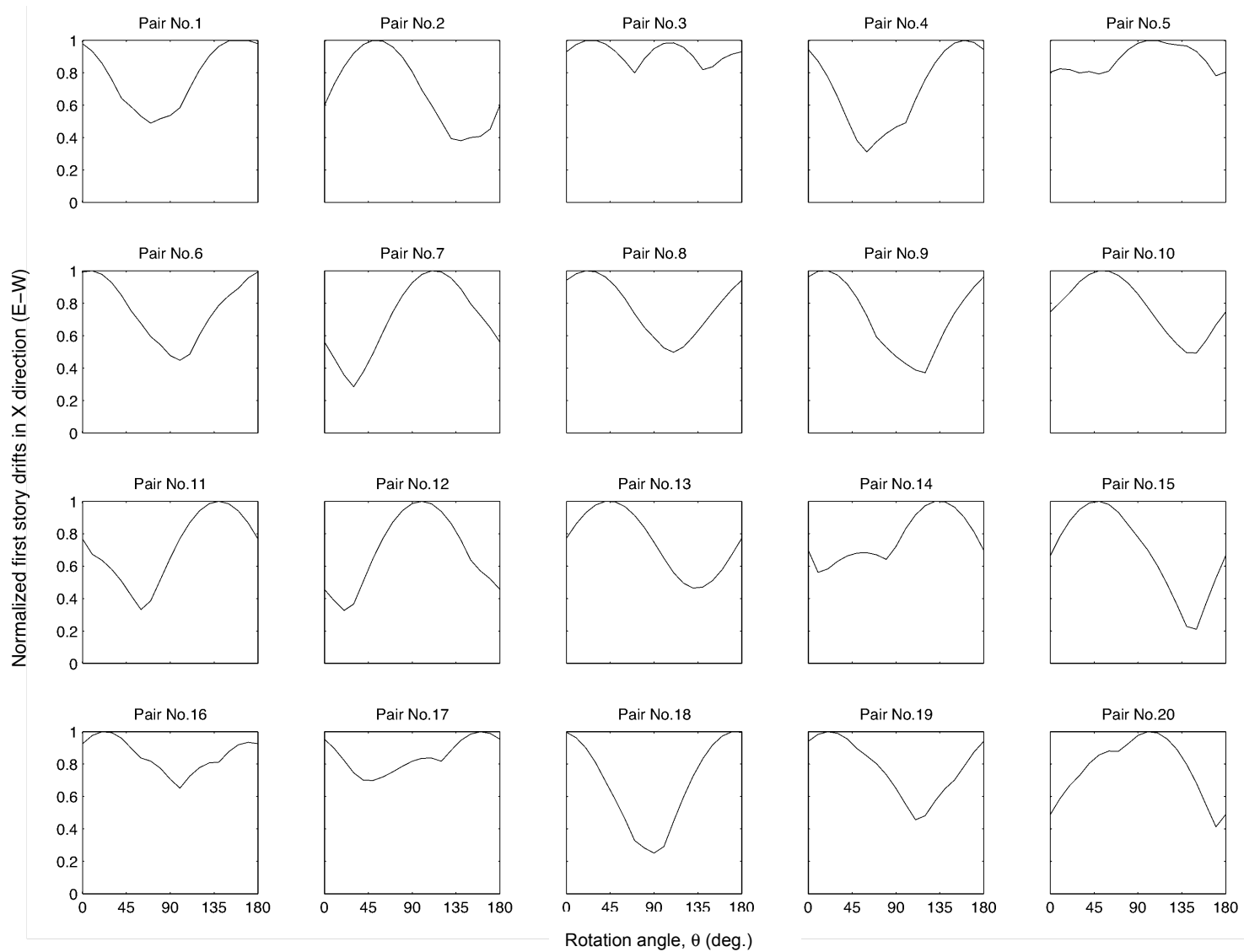


Figure 5. Normalized first story drift in longitudinal direction (X or E-W) as a function of clockwise rotation angle θ for twenty ground motion pairs. The normalizing factor is the maximum value over all angles for the ground motion pair being considered; this factor differs for each pair. This figure shows that story drift can vary by a factor of 2 over the possible angles of interest [Note: FN directions is not necessarily at 0°].

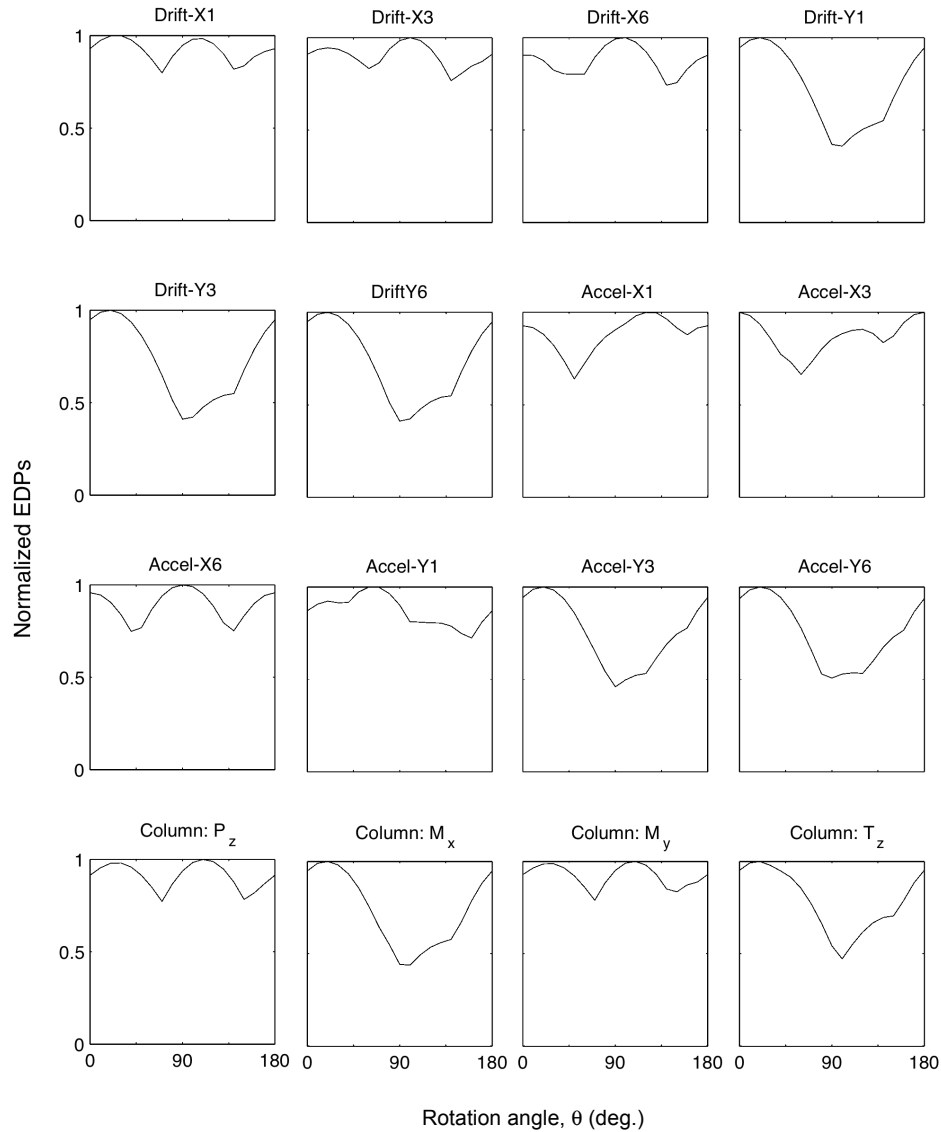


Figure 6. For ground motion Pair No. 3, normalized Engineering Demand Parameters (EDPs) show different degree of variation with respect to clockwise rotation angle θ . In this figure, P_z , M_x , M_y , and T_z correspond to the first-story corner column's axial force, moments about two orthogonal directions and torsion; number following X- or Y-direction indicates the floor, for example Accel-X6 means 6th floor acceleration along the X-direction [Note: FN directions is not necessarily at 0°].

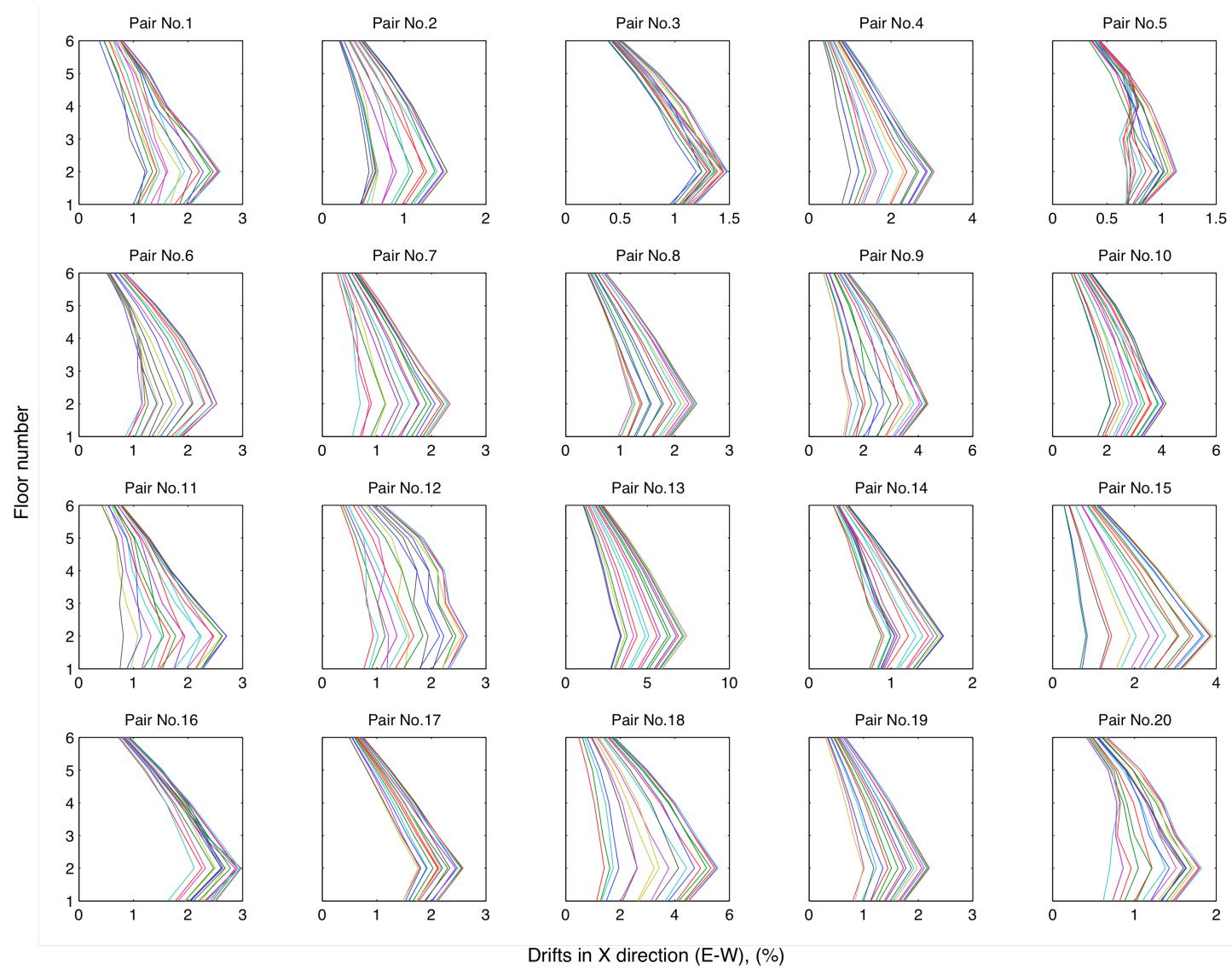


Figure 7. Story drift profiles in longitudinal (X or E-W) direction for twenty ground motion pairs rotated 0° through 180° clockwise with an interval of 10° . In order to illustrate the relative variability with respect to the rotation angle, a common scale was not used.

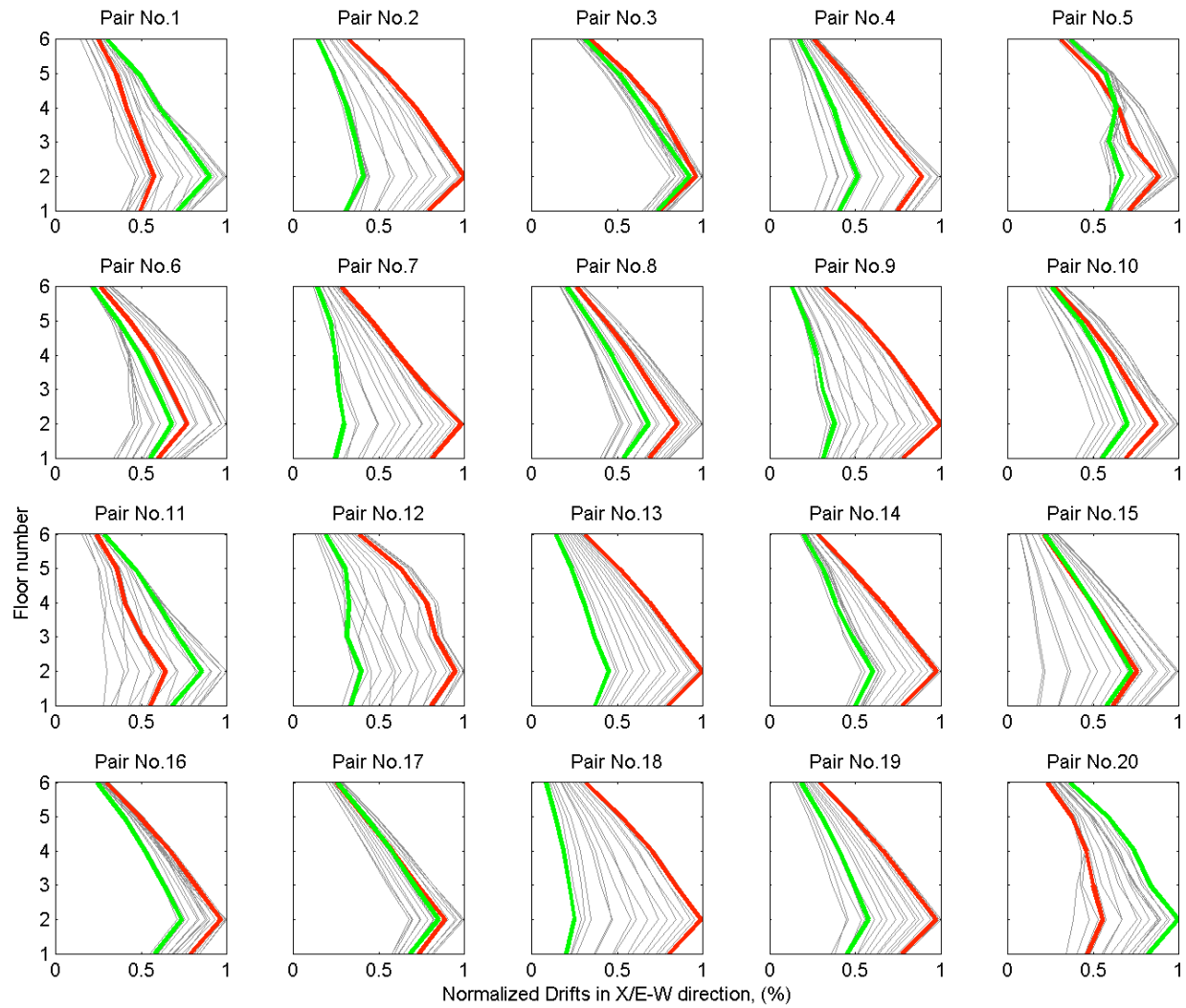


Figure 8. Story drift profiles in longitudinal (X or E-W) direction. Angles corresponding to the fault-normal and fault-parallel directions shown in red and green, respectively.

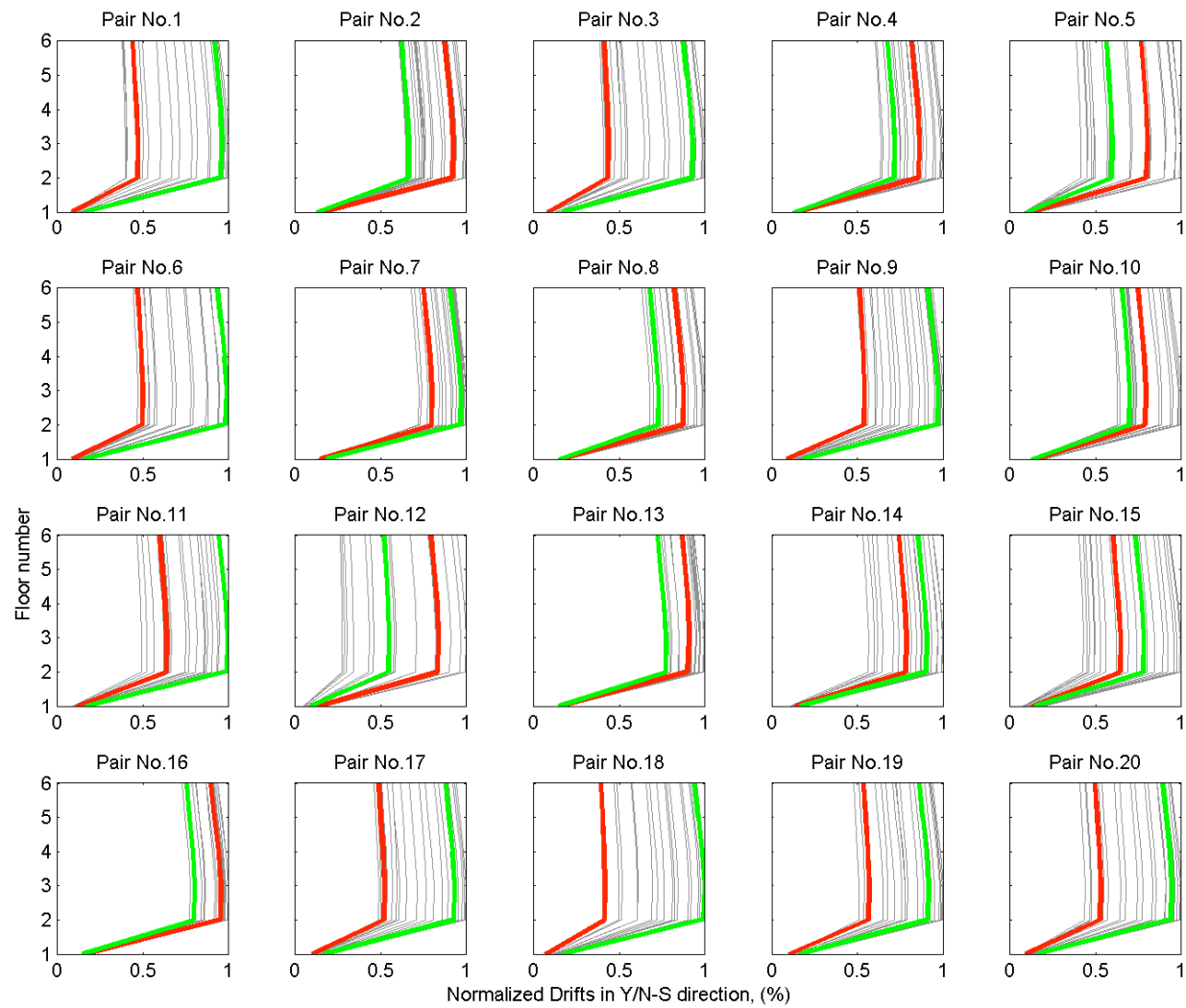


Figure 9. Story drift profiles in transverse (Y or N-S) direction. Angles corresponding to the fault-normal and fault-parallel directions shown in red and green, respectively.

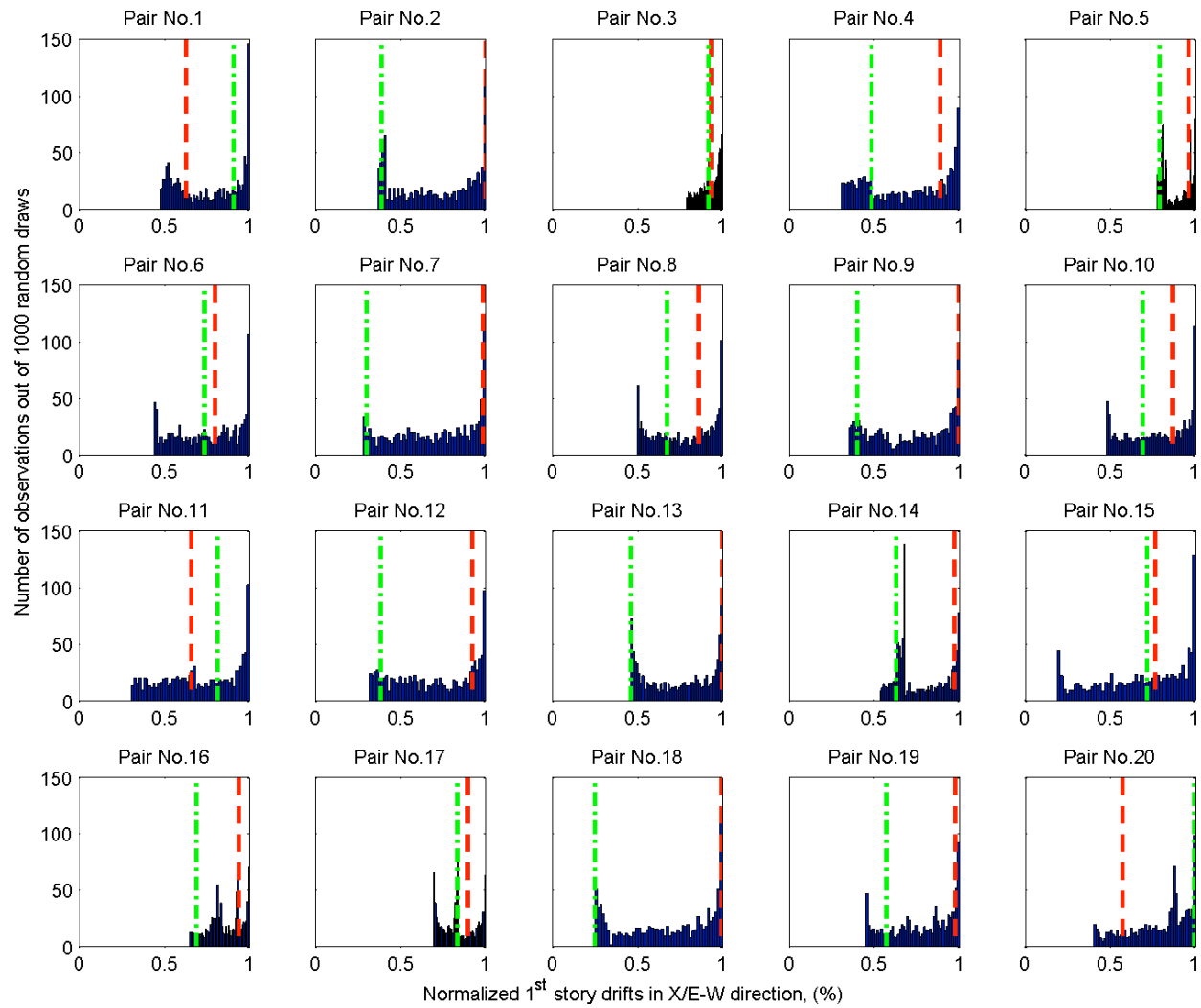


Figure 10. Histogram of 1,000 randomly obtained realizations of first story drift in X-direction. The red line indicates the value corresponding to the fault-normal direction, while the green line indicates that corresponding to the fault-parallel direction.

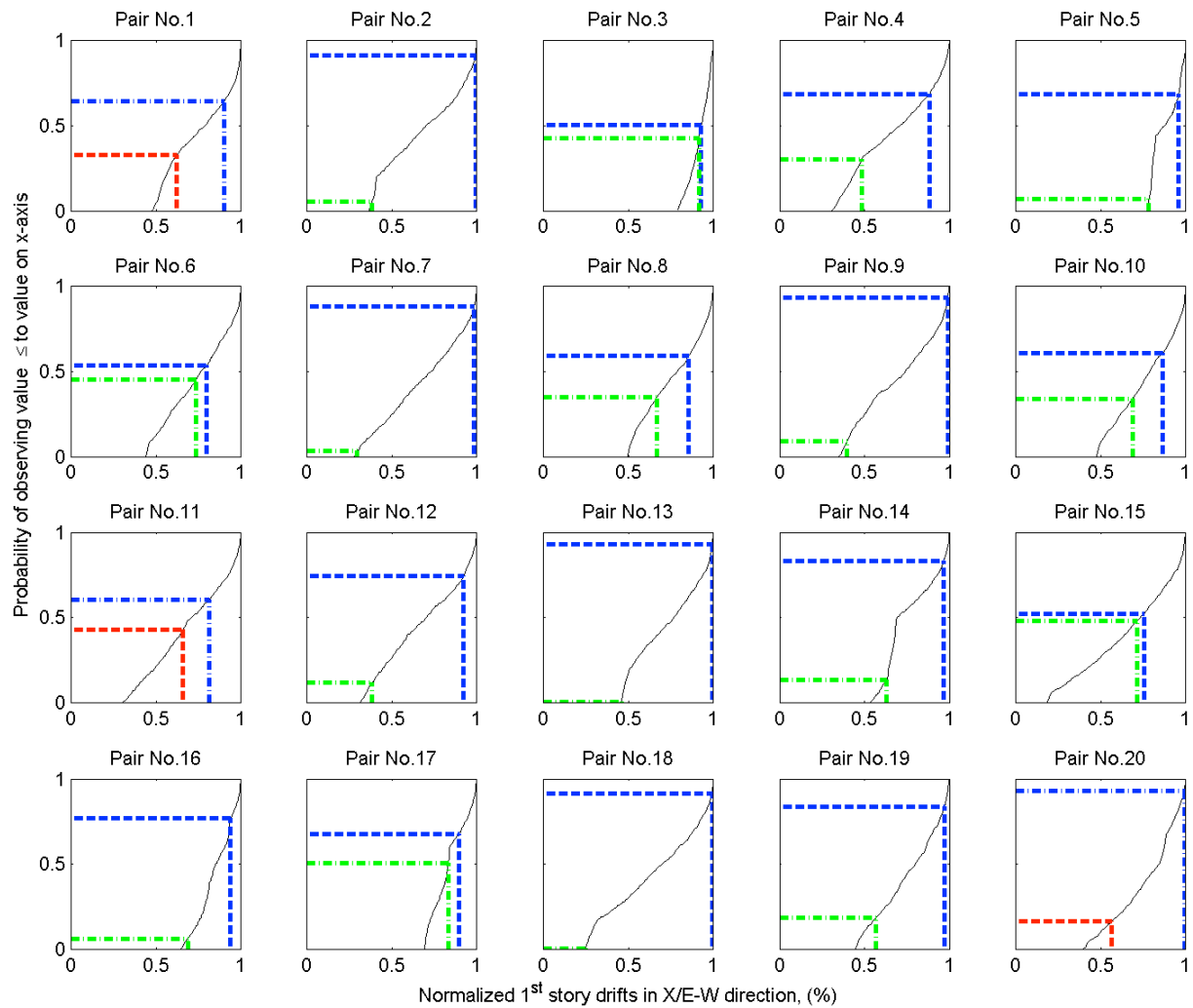


Figure 11. For a given pair of ground motion and a given value of first-story drifts in X-direction, the probability of observing an EDP value equal to or less than the given EDP value is shown based on 1,000 realizations. The red line indicates the EDP value corresponding to the fault-normal direction while the green line indicates that corresponding to the fault-parallel direction. The blue line indicates the larger of FN/FP responses.